Palaeontology
The Palaeontological Association
www.palass.org
[Palaeontology, 2023, e12670]

# What's inside a sauropod limb? First three-dimensional investigation of the limb long bone microanatomy of a sauropod dinosaur, *Nigersaurus taqueti* (Neosauropoda, Rebbachisauridae), and implications for the weight-bearing function

*by* RÉMI LEFEBVRE[1]*, RONAN ALLAIN[2] *and* ALEXANDRA HOUSSAYE[1]

[1]Mécanismes Adaptatifs et Évolution, UMR 7179, MNHN, CNRS, Muséum national d'Histoire naturelle, 55 rue Buffon, CP55, Paris 75005, France, remi.lefebvre1@mnhn.fr, alexandra.houssaye@mnhn.fr
[2]Centre de Recherche en Paléontologie – Paris, UMR 7207, MNHN, SU, CNRS, Muséum national d'Histoire naturelle, 8 rue Buffon, CP38, Paris 75005, France, ronan.allain@mnhn.fr
*Corresponding author

Typescript received 19 January 2023; accepted in revised form 12 June 2023

**Abstract:** Various terrestrial tetrapods convergently evolved to gigantism (large body sizes and masses), the most extreme case being sauropod dinosaurs. Heavy weight-bearing taxa often show external morphological features related to this condition, but also adequacy in their limb bone inner structure: a spongiosa filling the medullary area and a rather thick cortex varying greatly in thickness along the shaft. However, the microanatomical variation in such taxa remains poorly known, especially between different limb elements. We highlight for the first time the three-dimensional microstructure of the six limb long bone types of a sauropod dinosaur, *Nigersaurus taqueti*. Sampling several specimens of different sizes, we explored within-bone, between-bones, and size-related variations. If a spongiosa fills the medullary area of all bones, the cortex is rather thin and varies only slightly in thickness along the shaft. Zeugopod bones appear more compact than stylopod ones, whereas no particular differences between serially homologous bones are found. *Nigersaurus*' pattern appears much less extreme than that in heavy terrestrial taxa such as rhinoceroses, but is partly similar to observations in elephants and in two-dimensional sauropod data. Thus, microanatomy may have not been the predominant feature for weight-bearing in sauropods. External features, such as columnarity (shared with elephants) and postcranial pneumaticity, may have played a major role for this function, thus relaxing pressures on microanatomy. Also, sauropods may have been lighter than expected for a given size. Our study calls for further three-dimensional investigations, eventually yielding a framework characterizing more precisely how sauropod gigantism may have been possible.

**Key words:** bone microanatomy, graviportal, Sauropodomorpha, x-ray microtomography, functional morphology, biomechanics.

TERRESTRIAL gigantism appeared several times in the evolutionary history of tetrapods, such as in large proboscideans, rhinocerotoids, dicynodonts, ornithischians, theropods and sauropods (Alexander 1998; Sander & Clauss 2008; Sulej & Niedźwiedzki 2019; Hutchinson 2021), reaching a multi-tonne body mass. These forms, often said to be 'graviportal', show morphological features in their limb bones related to the support of a heavy weight, such as straightened and/or robust bones, depending on the taxon, but also proximal elements proportionately longer than distal ones (Gregory 1912; Osborn 1929; Coombs 1978; Hildebrand 1982; Carrano 2001, 2005; Christiansen 2007; Mallet *et al.* 2019; Hutchinson 2021; Lefebvre *et al.* 2022).

Their microanatomy (i.e. the inner architecture constituting the bone) also shows adequacy with a heavy-weight support role, since heavy quadrupedal taxa tend to show an increase in compactness, with a medullary area filled by a spongiosa often associated with a thickening of the cortex (Wall 1983; Houssaye *et al.* 2016; Nganvongpanit *et al.* 2017 fig. 1). Those trends are also found, maybe to a lesser extent, in gigantic bipeds such as large theropods, with a thickening of the cortex and sometimes a spongiosa partly filling the shaft (see Fabbri *et al.* 2022, extended data figs 1, 2, 8, 10). Microanatomical features associated to heavy-weight bearing are thought to be related to resistance to compressive loading, avoiding crushing fractures by improving energy absorption when


doi: 10.1111/pala.12670

the limb impacts the ground (Oxnard 1990; Augat & Schorlemmer 2006; Houssaye *et al.* 2016, 2021). This condition contrasts with more lightly built terrestrial tetrapods that show a tubular organization with an open medullary cavity, with spongious bone restricted to the metaphyses and epiphyses (Wall 1983 fig. 2; Oxnard 1990; Canoville & Laurin 2010; Houssaye *et al.* 2018).

However, little is known about microanatomical patterns in sauropod limb bones, notably due to their large size rendering them hardly available for appropriate sampling. Many studies have focused on the histology (i.e. the study of the nature of osseous tissues), especially of limb bones, to address questions about sauropod growth patterns and metabolism (e.g. de Ricqlès 1983; Curry 1999; Sander 2000; Klein & Sander 2008; Mitchell & Sander 2014; Curry Rogers *et al.* 2016; Cerda *et al.* 2017; Cerda. 2022), insular dwarfism (e.g. Sander *et al.* 2006; Stein *et al.* 2010), exceptional preservation of cartilage (e.g. Schwarz *et al.* 2007) and palaeopathology (e.g. González *et al.* 2017; Jentgen-Ceschino *et al.* 2020). For this purpose, partial cross-sections and core-drillings (Sander 2000), more easily obtainable for such large specimens, were sufficient, whereas microanatomical studies, which address the distribution of the osseous tissues in the bone, rather require complete cross-sections. Particular interest has also been cast on the microanatomy and histology of other postcranial elements, especially regarding axial pneumaticity (e.g. Wedel 2003, 2005 Cerda *et al.* 2012; Yates *et al.* 2012; Aureliano *et al.* 2021), cervical (e.g. Klein *et al.* 2012a; Cerda 2022) and dorsal ribs (e.g. Woodward & Lehman 2009; Waskow & Sander 2014), or osteoderms (e.g. Curry Rogers *et al.* 2011; Cerda *et al.* 2015; Vidal *et al.* 2017; Cerda 2022).

Although studies have investigated or illustrated one or several entire transverse sections of sauropod stylopod and zeugopod bones (Hatcher 1901; Ostrom & McIntosh 1966; de Ricqlès 1983; Rimblot-Baly *et al.* 1995; Galton 2005; Wings *et al.* 2007; Ye *et al.* 2007; Woodward & Lehman 2009; Company 2011; Sander *et al.* 2011; Klein *et al.* 2012b; Hedrick *et al.* 2014; Mitchell & Sander 2014; Curry Rogers *et al.* 2016; Ghilardi *et al.* 2016; Houssaye *et al.* 2016; Curry Rogers & Kulik 2018; González *et al.* 2020) and could be of interest for studying microanatomy, this gives an incomplete and poorly intercomparable overview of the sauropod limb long bones' inner structure. Microanatomy indeed varies for the same bone between various specimens of a same species, but also between the different bones of a single individual (Currey & Alexander 1985; Laurin *et al.* 2011; Amson & Kolb 2016; Houssaye & Botton-Divet 2018; Legendre & Botha-Brink 2018; Canoville *et al.* 2022) and can even greatly vary along the shaft of a single bone (Wall 1983; Nakajima *et al.* 2014; Waskow & Sander 2014; Houssaye *et al.* 2015; Amson 2021). Such within-bone variation is notably related to the position of the growth centre (GC), corresponding to the point where growth originated (Houssaye *et al.* 2015). Its longitudinal level can be estimated by the position along the shaft where the cortex is the thickest (Nakajima *et al.* 2014; Houssaye *et al.* 2015, 2021; Houssaye & Prévoteau 2020). It constitutes a biologically homologous point of comparison across species, but its position along the shaft can greatly vary between taxa and between bones (turtle humeri, Nakajima *et al.* 2014; mammalian humeri and femora, Houssaye *et al.* 2015, 2021; Houssaye & Botton-Divet 2018; Houssaye & Prévoteau 2020). Therefore, geometrically homologous transverse sections, usually taken at midshaft (which does not necessarily constitute a biologically homologous area) may not necessarily be suitable for biological comparisons.

Intra-individual skeletal variations can reflect paramount biomechanical implications. Indeed, differences in cortical and trabecular features may be the response to differential mechanical stresses experienced by limb bones, during locomotion and even during standing at rest (Currey & Alexander 1985; Oxnard 1990; Amson & Kolb 2016; Houssaye *et al.* 2016). They can reflect size (and mass)-related differences of forces involved in biomechanical stressful events, such as foot impact (Warner *et al.* 2013), and variability in loading experienced during locomotion (Willie *et al.* 2020), although this signal may be mixed with those associated with jointly active pressures, such as mass saving (Currey & Alexander 1985; Amson & Kolb 2016). However, this intra-individual variation has scarcely been documented, given the difficulty in making longitudinal sections (e.g. Wall 1983), but is now increasingly investigated with the advent of x-ray microtomography, allowing the creation of virtual sections of a digitized bone (e.g. Nakajima *et al.* 2014; Houssaye & Botton-Divet 2018; Amson 2021). To our knowledge, Curry Rogers *et al.* (2016) provided the first illustration of sauropod longitudinal sections of stylopodial (humerus, femur), zeugopodial (tibiae, fibulae) and autopodial (metacarpal III, metatarsal I) elements of a perinate specimen of the titanosaur *Rapetosaurus krausei*. However, this study focused on the histology and growth pattern of this sauropod, and hence did not describe the bone microanatomy.

Here we provide the first three-dimensional microanatomical investigation of a sauropod, using the rebbachisaurid sauropod *Nigersaurus taqueti* (Sereno *et al.* 1999, 2007). By studying for the first time the six types of limb long bone of several individuals varying in size, we aim to determine the microanatomical pattern occurring in this sauropod. This will highlight: (1) intra-bone; (2) -between-bones; and (3) size-related variations; thus allowing a discussion of limb long bone microanatomical adaptation to biomechanical constraints in this taxon.

**TABLE 1.** Measurements of material sampled in this study.

| Collection number | Bone | Orientation | Resolution (μm) | ML (cm) | Completeness of Scan | CEI MS | CEI GC |
|---|---|---|---|---|---|---|---|
| MNHN.F.GDF2097 | H | L | 86 | 26.7 | Complete | 0.51 | 0.53** |
| MNHN.F.GDF242.1 | H | R | 113 | 46.1 | Complete | / | / |
| MNHN.F.GDF243 | H | L | 97 | 48.3 | Shaft only | 0.59* | 0.58* |
| MNHN.F.GDF2045 | H | R | 96 | (Incomplete) | Shaft only | 0.63* | 0.61* |
| MNHN.F.GDF242.2 | R | R? | 124 | 32.8 | Complete | 0.77* | 0.77* |
| MNHN.F.GDF2057 | R | L | 94 | (Incomplete) | Shaft only | 0.73* | 0.73* |
| MNHN.F.GDF242.3 | U | R | 94 | 36.6 | Complete | 0.73*,** | 0.73*,** |
| MNHN.F.GDF75 | Fm | R | 97 | 40.6 | Complete | 0.52 | 0.55 |
| MNHN.F.GDF327 | Fm | R | 105 | 75.8 | Shaft only | 0.59*,** | 0.59*,** |
| MNHN.F.GDF2094 | T | R | 88 | 26.8 | Complete | 0.68* | 0.70* |
| MNHN.F.GDF244 | T | L | 97 | 51.8 | Shaft only | 0.70* | 0.64*,** |
| MNHN.F.GDF2095 | Fb | R | 86 | 27.9 | Complete | 0.63* | 0.67* |
| MNHN.F.GDF2055 | Fb | R | 93 | 51.1 | Shaft only | 0.77*,** | 0.80*,** |

*Abbreviations*: CEI, cortical extension index; GC, growth centre section; ML, bone maximum length (cm); MS, midshaft section; *Bone*: H, humerus; R, radius; U, ulna; Fm, femur; T, tibia; Fb, fibula; *Orientation*: left (L) or right (R) bone; / section too incomplete to be confidently measured.

*Unclear delineation of the cortex.

**Estimation relying on reconstructed parts or involving discontinuities due to incompleteness.

Given the outcomes of previous studies made on heavy-weight bearing taxa (Wall 1983; Houssaye *et al.* 2016), we expect to find in all *Nigersaurus* limb long bones a marked thickening of the cortex along the shaft, and a spongiosa filling the medullary area. Since the body centre of mass is inferred to be posteriorly placed in most diplodocoid sauropods (Henderson 2006), we may also expect to find a substantial difference in the microanatomical pattern between forelimb and hindlimb bones (i.e. hindlimb microanatomy bulkier than forelimb one). Consistently with Amson & Kolb (2016) who suggested less pressure related to mass saving on zeugopod bones than on stylopod bones, which hence probably reflect more pressure related to biomechanical stresses for the zeugopods, we expect to find a more robust pattern in the radius and ulna compared to the humerus, and in the tibia and fibula with respect to the femur.

## MATERIAL AND METHOD

### *Material*

We studied 13 limb bones (four humeri, two radii, one ulna, two femora, two tibiae and two fibulae; see Table 1) referred to the sauropod *Nigersaurus*. This elephant-sized sauropod (Sereno *et al.* 2007) is known from several bones representing several specimens of various sizes, collected in Aptian–Albian deposits of Gadoufaoua, Elhraz Formation, Niger (Taquet 1976). Although initially diagnosed as a 'dicraeosaurid titanosaur' (Taquet 1976), this material was later attributed as a diplodocoid belonging to the more recently erected Rebbachisauridae family, within the species *Nigersaurus taqueti* (Sereno *et al.* 1999). Moreover, this material was compared to the type and referred material of *Nigersaurus taqueti* (Sereno *et al.* 1999, 2007), examined at first hand by one of us (RA). The bones sampled here were selected for their completeness, the quality of their preservation, and with the concern to cover the largest possible size range available (sampling the largest and smallest individuals available when possible; Table 1). Three bones from a single forelimb belong with certainty to the same individual (MNHN.F.GDF242), and two hindlimb zeugopod are reasonably associated to the same individual (MNHN.F.GDF2094 & 2095). These specimens are housed in the palaeontological collections of the Muséum national d'Histoire naturelle, Paris, France (MNHN).

### *Methods*

Bones were scanned with high-resolution computed tomography (GEphoenix|X-ray v|tome|xs 240) at the AST-RX platform (UMS 2700) of the MNHN; reconstructions were performed using datox/res software. Image visualizations and virtual sections were performed using VGStudioMax v.2.2 (Volume Graphics Inc., Heidelberg, Germany). The resolution of the scans depended of the size of the specimens (the larger the specimen, the larger the resolution). Virtual sections were made in the coronal and sagittal planes crossing the middle of the shaft with the bones oriented so that the midshaft region is vertical. In addition, virtual transverse sections were

made at midshaft, permitting analogous comparisons with transverse sections widely encountered in the literature as made in the reference plane, and another at the estimated position of the GC, where the cortex is the thickest, in order to produce biologically homologous sections, since bone microanatomy can strongly vary along the shaft, and since the GC is rarely at midshaft (Nakajima *et al.* 2014; Houssaye & Prévoteau 2020). In these transverse sections, we measured the proportion of the total cross-sectional area occupied by the cortex. It estimates quantitatively the overall cortical thickness of the section. This cortical extension index (CEI) is a ratio calculated as follows: CEI = 1 – ((Medullary area)/(Sectional area)). Area measurements were performed using the polyline and measurement tools in the software ImageJ v.1.53a (Schneider *et al.* 2012). Due to the incompleteness of some sections, this measurement was based on the plaster-reconstructed parts of the bones when they occur, since they appeared to follow the whole geometry of the original bone, without extrapolations. When these reconstructions were missing, a straight line was traced to estimate the missing portion. As the delineation between the cortex and the spongiosa is sometimes unclear, all CEI estimations were taken three times and averaged to account for any potential measurement error. The maximum length (ML) was virtually measured on 3D models of the bones using the Meshlab software (Cignoni *et al.* 2008). Illustrated virtual sections were luminosity-inverted and, when relevant, manually contrast-adjusted using Inkscape software.

## RESULTS

### *Humerus*

In the sampled humeri, the medullary area is totally filled by a spongiosa made of thin and numerous osseous trabeculae (Fig. 1A–F). The GC is located slightly below the midshaft level (Fig. 1A–C). The cortex is rather thin, even near the GC, where it is slightly thicker. The CEI slightly differs between the smallest (about 50% in MNHN.F.GDF2097; Table 1; Fig. 1D) and the largest (around 60%, in MNHN.F.GDF243 & 2045; Table 1; Fig. 1E) specimens, whatever the type of transverse section observed.

### *Radius*

In the sampled radii, the medullary area is relatively smaller and thus the cortex relatively thicker in the shaft region than in the humerus, and is totally filled by a spongiosa (Fig. 1G–H, J–K). The osseous trabeculae are thin and numerous as in the humerus, but the density of the spongiosa diminishes towards the core of the shaft. The GC is located around midshaft (MNHN.F.GDF242.2; Fig. 1H), though its precise position is unclear since the associated localized thickening of the cortex is rather gradual. Transversally the cortex is thicker anterolaterally and posteromedially (MNHN.F.GDF2057, Fig. 1J; unclear in MNHN.F.GDF242.2 due to poor preservation). The CEI ranges between 73% and 77% (Table 1).

### *Ulna*

In the sampled ulna (Fig. 1I, L), the bone microanatomy is similar to that of the radius. The GC is located around midshaft (Fig. 1I). The cortical thickening around the GC is more acutely marked than in the humerus and the radius. At the GC, the cortex is thicker posteriorly than mediolaterally (Fig. 1I, L; CEI is estimated around 73%; Table 1). Due to incompleteness, it is not possible to know if the cortex is anteriorly as thick as posteriorly.

### *Femur*

The osseous trabeculae of the sampled femora are thin and numerous (Fig. 2A–B, D–E). The spongiosa is present in the majority of the medullary area of the smallest specimen (MNHN.F.GDF75; Fig. 2A, D). It is, however, not totally clear if the medullary area of the smallest specimen was entirely filled in the midshaft region, due to taphonomic alterations. The spongiosa totally fills the medullary area in the largest specimen (MNHN.F.GDF327; Fig. 2B, E), with no medullary cavity. The GC is slightly below the midshaft in the smallest specimen (MNHN.F.GDF75; Fig. 2A) and around the midshaft in the largest specimen (Fig. 2B). In the smallest specimen (Fig. 2A), the structures at midshaft and near the GC are similar, and the cortical thickness is roughly homogeneous along the sections. The CEI in the small

**FIG. 1.** Virtual sections of *Nigersaurus* forelimb elements. A–F, humeri; G–H, J–K, radii; I, L, ulna. A, D, MNHN.F.GDF2097 in: A, coronal; D, transverse (near the growth centre (GC)) view. B, E, MNHN.F.GDF2045 in: B, coronal; E, transverse (near the GC) view. C, F, MNHN.F.GDF242.1 in: C, coronal; F, transverse (near the GC) view. G, J, MNHN.F.GDF2057 in: G, coronal; J, transverse (slightly below the GC) view. H, K, MNHN.F.GDF242.2 in: H, coronal; K, transverse (near the GC) view. I, L, MNHN.F.GDF242.3 in: I, coronal; L, transverse (near the GC) view. Asterisks denote the estimated GC location. Scale bars represent: 4 cm (A–C, G–I); 1 cm (D–F, J–L).

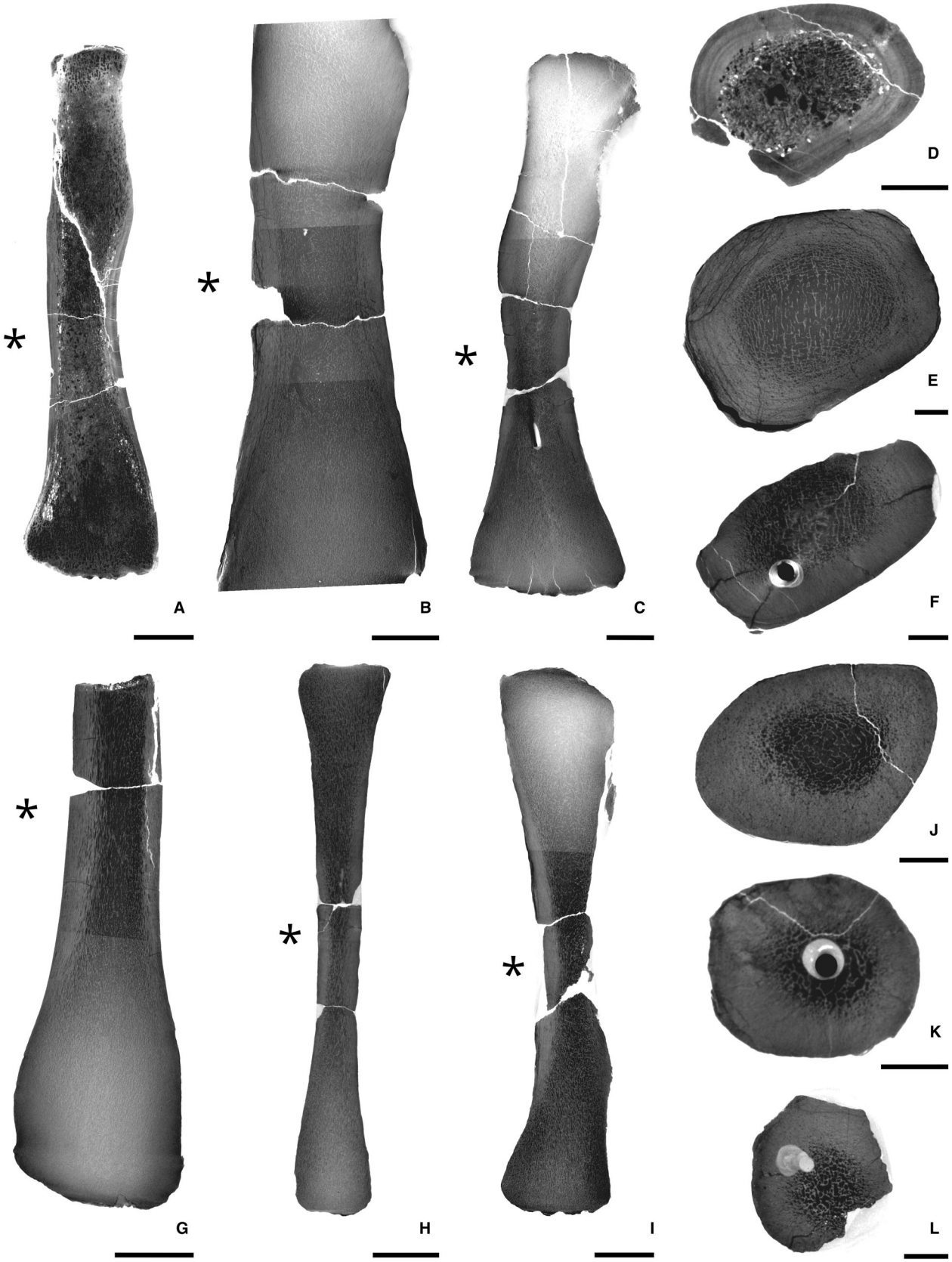

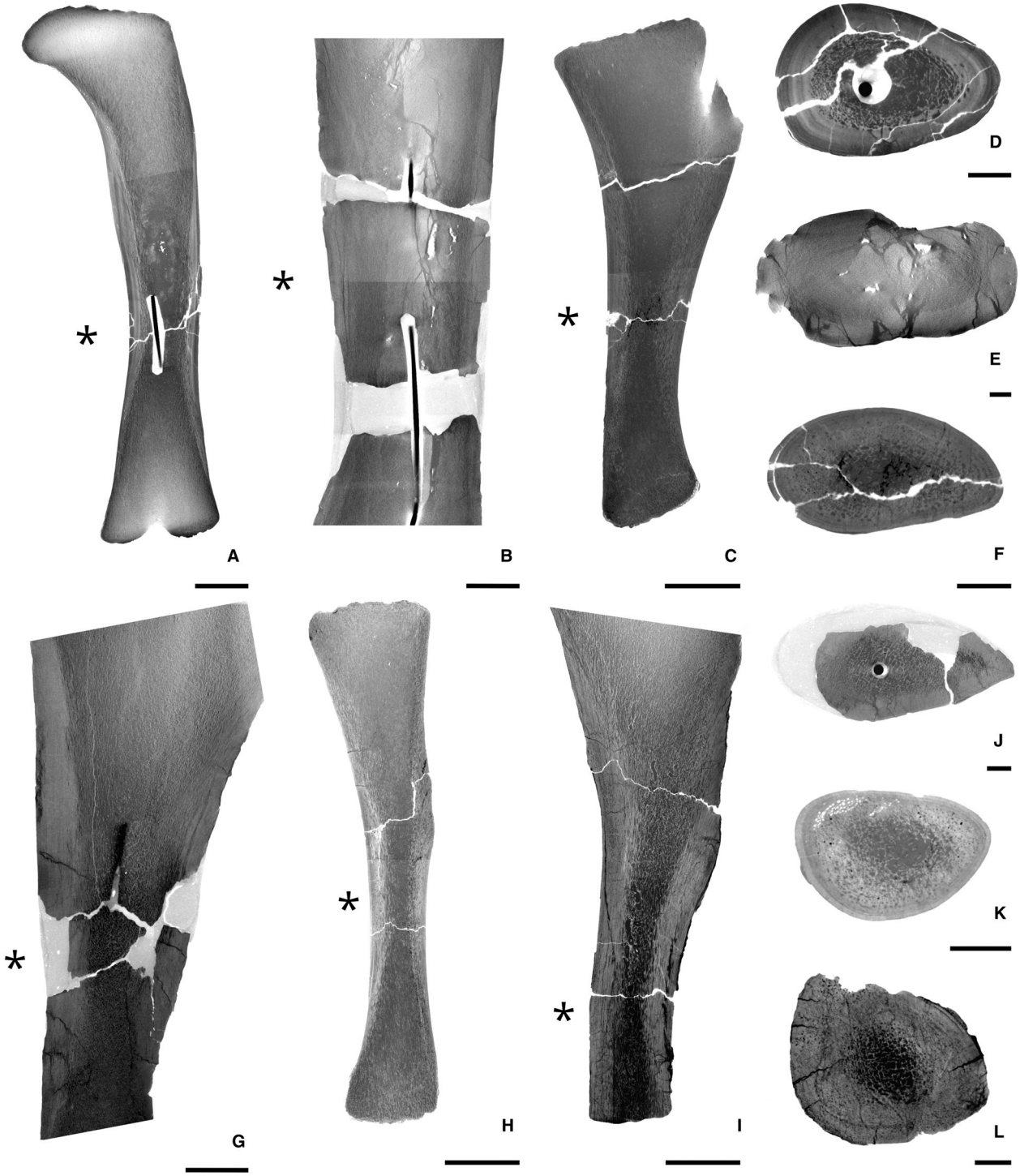


**FIG. 2.** Virtual sections of *Nigersaurus* hindlimb elements. A–B, D–E, femora; C, F–G, J, tibiae; H–I, K–L, fibulae. A, D, MNHN.F.GDF75 in: A, coronal; D, transverse (near the GC) view. B, E, MNHN.F.GDF327 in: B, coronal; E, transverse (near the GC) view. C, F, MNHN.F.GDF2094 in: C, coronal; F, transverse (near the GC) view. G, J, MNHN.F.GDF244 in: G, coronal; J, transverse (near the GC) view. H, K, MNHN.F.GDF2095 in: H, coronal; K, transverse (near the GC) view. I, L, MNHN.F.GDF2055 in: I, coronal; L, transverse (near the GC) view. Asterisks denote the estimated GC location. Scale bars represent: 4 cm (A–C, G–I); 1 cm (D–F, J–L).

specimen is lower (between 52% and 55%, Table 1; Fig. 2D) than in the large specimen (CEI estimated around 59%; Table 1; Fig. 2E).

### *Tibia*

In the sampled tibiae, the osseous trabeculae are thin and numerous (Fig. 2C, F, G, J). In the small specimen (MNHN.F.GDF2094; Fig. 2C, F), trabecular density is lower in the core of the medullary area especially above the GC. The trabecular density is homogeneous along the shaft in the large specimen (MNHN.F.GDF244; Fig. 2G, J). The GC is located below the midshaft (Fig. 2C, G). The spongiosa is slightly denser in this region in the large specimen than in the small one. The cortex is proportionally thicker than in the humerus and the femur, with a CEI around 64–70%, whichever section or specimen is considered (Table 1; Fig. 2F, J). The cortical thickening around the GC is as marked as in the ulna. The cortex is proportionally thicker posteriorly, especially in the largest specimen (Fig. 2G).

### *Fibula*

In the sampled fibulae (Fig. 2H, I, K, L), the bone microanatomy is similar as in the tibiae, with a trabecular density lower in the core (in the small specimen MNHN.F.GDF2095; Fig. 2H, K) to homogeneous (in the large specimen MNHN.F.GDF2055; Fig. 2I, L) in the medullary area. The osseous trabeculae are thin and numerous. The GC is located below the midshaft (Fig. 2H, I). The CEI in the large specimen is thicker (77–80%; Table 1; Fig. 2L) than in the small one (63–67%; Table 1; Fig. 2K), both are hence thicker than in the humerus and the femur.

## DISCUSSION

### *Microanatomical pattern in* Nigersaurus

The limb long bone microanatomy of *Nigersaurus* is characterized by a rather thin cortex and a spongiosa partially to totally filling the medullary area. The CEI of *Nigersaurus* stylopod bones varies between 50% and 60%. These values are relatively low when compared with other large terrestrial animals (CEI ranges from 43% in a juvenile *Apatosaurus* to 93% in the black rhinoceros *Diceros bicornis*; see Table 1 & Table S1). The extension of the spongiosa in the shaft is observed in many other terrestrial heavy-weight bearing taxa (proboscideans, rhinoceroses, sauropods; see Wall 1983; Curtin *et al.* 2012; Curry Rogers *et al.* 2016; Houssaye *et al.* 2016; Nganvongpanit *et al.* 2017), whereas lighter ones show an open medullary cavity (e.g. giraffe, buffalo, bison in Wall 1983 and Houssaye *et al.* 2016). The extension of the spongiosa as a dense mesh of thin and numerous trabeculae observed in *Nigersaurus* is also found in the shaft of rhinoceroses (Wall 1983; Houssaye *et al.* 2016; AH & C. Etienne, pers. comm. 2022), hippopotamuses (Houssaye *et al.* 2021), the ceratopsid *Centrosaurus* (Houssaye *et al.* 2016), the thyreophoran *Stegosaurus* (Ostrom & McIntosh 1966; Houssaye *et al.* 2016) and many sauropods (e.g. Ostrom & McIntosh 1966; Rimblot-Baly *et al.* 1995; Hedrick *et al.* 2014; Mitchell & Sander 2014; Curry Rogers *et al.* 2016; González *et al.* 2020) but also in some xenarthrans (Straehl *et al.* 2013; Amson *et al.* 2014; Amson & Nyakatura 2018). Thin and numerous trabeculae are also observed in the limb long bones of the Asian elephant *Elephas maximus* (see Nganvongpanit *et al.* 2017), but the midshaft sections of extant elephants in Houssaye *et al.* (2016) show fewer and thicker trabeculae, suggesting possible variation among modern elephants.

*Variation within bone.* A posterior asymmetrical thickening of the cortex is seen in the ulna, tibia and fibula (Figs 1I, 2C, F, G, H–I, K–L). It has been suggested that the curvature of the ulna in terrestrial mammals was optimized to counterbalance the stresses caused by the extension of the triceps (Milne 2016). This condition is also seen in sauropods (Lefebvre *et al.* 2022), and the posterior inner reinforcement seen in the ulna may be correlated to this external condition. Bone microanatomy varies only slightly along the shaft in *Nigersaurus*, compared with the condition seen in rhinos, and some bones of elephants and *Rapetosaurus*, in which an abrupt thickening at the level of the GC is observed longitudinally (Wall 1983; Curry Rogers *et al.* 2016; Nganvongpanit *et al.* 2017; AH & C. Etienne, pers. comm. 2022). In *Nigersaurus*, longitudinal variation is, however, more marked in the smaller tibia (MNHN.F.GDF2094; Fig. 2C) and fibula (MNHN.F.GDF2095; Fig. 2H) by the presence of a slightly denser spongiosa near the GC. The difference of within-bone variability observed between longitudinal sections of *Nigersaurus* (in this study) and the hindlimb zeugopod of *Rapetosaurus* (Curry Rogers *et al.* 2016) suggests that thickening variability differs between sauropods and/or ontogenetic stages, and calls for the three-dimensional investigation of other species series in order to better understand the occurrence of these variations within this clade.

*Variation between bones.* As expected, the zeugopod bones of *Nigersaurus* are more compact than the stylopod ones (Table 1), suggesting relatively higher biomechanical pressure experienced by the radius, ulna, tibia and fibula

(Currey & Alexander 1985; Amson & Kolb 2016; Legendre & Botha-Brink 2018) during locomotion. This pattern has been noticed in several quadrupedal terrestrial taxa, such as Cervidae (Amson & Kolb 2016), tapirs (AH & G. Houée, pers. comm. 2020), and the aardvark *Orycteropus afer* (Legendre & Botha-Brink 2018). Canoville *et al.* (2022) recently noticed quite a similar trend in extant and extinct flightless birds. A larger-scale study based on diameter measurements (Currey & Alexander 1985) showed a highly consistent intraspecific trend in non-flying amniotes, with zeugopod bones almost always showing larger cortical occupation of the total diameter of the shaft than stylopod bones. This suggests that our observation is relatively ubiquitous in terrestrial animals, and is probably not linked to a heavy-weight bearing specialization. Thus, zeugopod microanatomy may generally be more constrained than stylopod microanatomy by weight-bearing biomechanical pressures in any terrestrial taxa. However, contrary to our expectations, no differences were found in the microanatomical pattern between forelimb and hindlimb serially homologous bones that could have reflected hindlimb elements bearing more weight than anterior ones.

*Size-related variation.* Two patterns related to the size of the specimens are observed: first, larger humeri, femora and fibulae tend to have a thicker cortex than smaller ones, and second, the trabecular density tends to increase in larger tibiae and fibulae. These two observations constitute a very plausible ontogenetic (i.e. growth) variation in *Nigersaurus*. However, a rather large intraspecific size variability at the same ontogenetic stage can occur in some sauropod taxa (Klein & Sander 2008; Mitchell & Sander 2014). In our study, since the magnitude of size variation in the sampled humeri, femora, tibiae and fibulae is large (*c.* 2 in each type of bone), we may reasonably favour the hypothesis that, for each type of those bones, at least the smallest and largest individuals correspond to two different ontogenetic stages (although alternative hypotheses such as sexual dimorphism (see discussion in Klein & Sander 2008) cannot be ruled out with our data). Functionally, these two observed size-related trends may be associated with the increase in body mass occurring during postnatal growth, and therefore would reflect an increase in the role of weight support at least in the hindlimb during this period. Such size-related variation might also occur in radii and ulnae, for which only one complete bone was available. Size-related cortical thickening is also found in flightless birds, and is probably associated with the regular bone growth through ontogeny (Canoville *et al.* 2022). This pattern is also found in two small ornithischian taxa (i.e. femur of *Dysalotosaurus*, Heinrich *et al.* 1993; tibia and fibula of *Jeholosaurus*, Han *et al.* 2020), which could suggest that this pattern is widespread at least among dinosaurs. The microanatomical data presented in this study highlight a very robust profile in the fibula, contrasting with the reduced presence of the fibula in a large number of terrestrial amniotes. This could indicate that this bone had a predominant role along with the tibia in order to support the body mass in *Nigersaurus*. However, the similar thickening observed in the small ornithischian *Jeholosaurus* (Han *et al.* 2020) may imply that this trend is widespread among non-avian dinosaurs, hence not particularly characteristic of heavy taxa. Size-related increase in trabecular density might also occur in humeri and femora, since the precise density of the smallest specimens is unclear due to preservation.

### *Implications for the weight-bearing function in sauropods*

Our results suggest that *Nigersaurus* shows some features expected to occur in association with a heavy-weight bearing biology, namely the presence of a spongiosa and a longitudinal cortical thickening along the shaft. However, this latter feature is only weakly marked, and the cortex is rather thin, compared to extant heavy mammals, notably rhinoceroses (see Wall 1983 fig. 2; Houssaye *et al.* 2016). One could argue that the not extreme condition of *Nigersaurus* could be linked to its relatively small size. However, this sauropod is about the size of an elephant (Sereno *et al.* 2007), which is the largest extant terrestrial animal. Moreover, although some elephant bones show an abrupt cortical thickening (see Nganvongpanit *et al.* 2017 fig. 1E), others show only a gradual thickening (see Nganvongpanit *et al.* 2017 fig. 1A, D), and even sometimes a medullary cavity (Curtin *et al.* 2012; Houssaye *et al.* 2016). This suggests that elephants do not necessarily show an extreme microanatomical condition, and exhibit features more similar to *Nigersaurus*.

A fairly high degree of microanatomical variability seems to be present across sauropod species, as suggested by transverse cross sections found in the literature. As in *Nigersaurus*, some other sauropods show a rather thin cortex, such as in the humeri of a small-sized *Ampelosaurus* individual and a juvenile specimen of *Apatosaurus* (see Houssaye *et al.* 2016). In contrast, the femur of a dwarf sauropod, *Magyarosaurus* (see Mitchell & Sander 2014), shows a very compact profile with a thick cortex. More surprisingly, a medullary cavity is found in the femora of very large taxa such as *Diplodocus* (see Hatcher 1901) and *Alamosaurus* (see Woodward & Lehman 2009), as well as in dwarf taxa such as *Europasaurus* and *Magyarosaurus* (see Mitchell & Sander 2014) suggesting that the presence of this feature may be not related to size. Assuming no taphonomic alterations, this overall variability seemingly poorly related to size is surprising,

occurring as it does across a sample representing all the major locomotor groups (Carrano 2005) within sauropods. This appears particularly inadequate with the assumed extreme biomechanical pressures that should have counter-selected such variability when associated with a multi-tonne body mass. This trend also seems inconsistent with the evolution in sauropodomorph dinosaurs of the filling of the medullary area by spongious bone, which, since it co-occurs with the emergence of Sauropoda (*sensu* Salgado *et al.* 1997; Cerda *et al.* 2017), appears to be strongly related to the evolution of their gigantism. Cerda *et al.* 2017 pointed out that such spongious bone infilling may have been retained in smaller and tardive sauropods through phylogenetic inertia. The evolution of this condition is perhaps even more complex since several sauropods of different sizes appear to display a medullary cavity partly or totally devoid of spongiosa. While the acquisition of a spongiosa filling the medullary area appears to be both biomechanically advantageous for weight-bearing (Oxnard 1990; Houssaye *et al.* 2016, 2021) and correlated with the emergence of the bauplan characterizing sauropods (see Lefebvre *et al.* 2022), this feature does not appear to be a *sine qua non* condition for the evolution of extremely large forms, such as *Alamosaurus* (see Woodward & Lehman 2009).

Therefore, the present study highlights the fact that the role of weight-bearing in *Nigersaurus*, as well as in a large number of the other sauropods examined here, probably depended less on microanatomy than in some other heavy-weight bearing extant mammals, such as rhinoceroses (Wall 1983; Houssaye *et al.* 2016), or some dinosaurs such as large thyreophorans (e.g. *Stegosaurus*; Houssaye *et al.* 2016). Considering the present study, two hypotheses, not exclusive to each other, emerge from these findings:

1. Microanatomical features were not predominant considering weight-bearing function in sauropods. Instead, a set of other features that are thought to be efficient in weight-bearing would have been sufficient in realizing this function, hence relaxing biomechanical (and probably selective) pressures on bone microanatomy. Those features include the presence of an (unpreserved) fleshy pad on the pes (Wilson 2005; Jannel *et al.* 2019, 2022), analogous to the condition seen in elephants (Weissengruber *et al.* 2006), that had a main role in energy absorption. Additionally, the existence of (rarely preserved; see Schwarz *et al.* 2007) cartilaginous epiphyses probably provided sauropods with better shock absorption and efficient mass support (Holliday *et al.* 2010; Bonnan *et al.* 2013; Tsai *et al.* 2020). Such cartilages accounted for a substantial part of the bone length (probably more than 10% according to Holliday *et al.* 2010, see also Bonnan *et al.* 2010; Vogoele *et al.* 2022) potentially impacting significantly biomechanical inferences made for such organisms (Schwarz *et al.* 2007; Mallison 2010; Bonnan *et al.* 2013; Tsai & Holliday 2014; Lefebvre *et al.* 2020; Voegele *et al.* 2022). Additionally, some size-related reinforcements in hindlimb bones shape (Lefebvre *et al.* 2022) constituted external features that may have participated to efficiently realize the weight bearing function. Finally, relatively relaxed microanatomy seems to be also observed in columnar-limbed elephants, since it is not unusual for some bones in some specimens to show a medullary cavity (Curtin *et al.* 2012; Houssaye *et al.* 2016; AH pers. obs. 2022). The congruence of this pattern seen in both groups hence suggests that the columnar limb architecture (Osborn 1900; Christiansen 2007) has a major, if not predominant, role in weight bearing, relaxing the necessity for microanatomical compensations to cope with extreme gigantism occurring in these organisms.
2. Sauropods were lighter than expected for a given size (i.e. not following mass/length proportionality principles; e.g. Alexander 1998). In other words, body mass of sauropods would have been increasing much slower than body length/height. Assuming this hypothesis, our study would provide reinforced support for studies tending to lower body mass estimations (e.g. Bates *et al.* 2015; Campione 2017; see Campione & Evans 2020 for a review) proposed for these taxa. Our assessment based here on microanatomy is congruent with morphological evidence highlighting the presence of a particularly well-developed postcranial pneumaticity (e.g. Wedel 2003; Cerda *et al.* 2012; Yates *et al.* 2012), which was supposed to significantly lighten the sauropod body (Wedel 2005). This is especially true for rebbachisaurids (Wilson & Allain 2015; Ibiricu *et al.* 2017), and particularly in the case of *Nigersaurus*, which is thought to have had an extremely lightly built skull and axial skeleton (Sereno *et al.* 2007). As postcranial pneumaticity participated to decrease constraints related to weight-bearing function, the evolution of this parameter probably had a critical influence on the evolution of limb long bone structure.

These two hypotheses should be tested through a larger exploration of limb bone microanatomy in massive terrestrial taxa. Although our study constitutes to our knowledge the largest documentation of the microanatomical pattern of entire limb long bones for a sauropod, the absolute size of our sample remains limited. Three-dimensional patterns seen in such large taxa are still extremely poorly documented, and our study calls for others to better delineate the evolutionary trends of microanatomical features in relation to heavy weight support. An integrative focus should be made on both

columnar (sauropods, elephants) and non-columnar (e.g. rhinoceroses, heavy ornithischians) taxa, ideally in a quantitative and phylogenetically-informed framework. Notably, a more exhaustive documentation of microanatomical diversity of sauropods should highlight the extent to which our conclusions can be generalized to the whole diversity within this clade.

Our results suggest that the degree of gigantism observed in extant terrestrial tetrapods (i.e. only represented by mammals) might not be fully analogous to the extreme condition seen in sauropods. The specificities related to their evolutionary history (particularly their cartilaginous epiphyses and well-developed pneumaticity) need to be taken into account to accurately infer how they evolved, perhaps by also addressing how the morphological traits of extant archosaurs scale with increasing size and increasing biomechanical pressures.

## CONCLUSION

The present study corresponds to the first three-dimensional investigation of the limb long bone microanatomy of a sauropod. The examination of *Nigersaurus*' longitudinal and transverse virtual sections permitted us to highlight a spongiosa partially or totally filling the medullary area, a trait classically associated with the support of a heavy body mass, and whose density appeared to vary with size in the tibia and the fibula. However, contrary to expectations, a rather thin cortex was found, only varying weakly in thickness along the shaft, contrasting with usually thick and abruptly varying cortices seen in heavy taxa. The cortex in zeugopod bones is proportionally thicker than in the stylopod ones, congruently with the literature, whereas no strong difference distinguishes the forelimb and the hindlimb serial homologues, despite the unequal distribution of the centre of mass (and, therefore, biomechanical constraints) in most sauropods. Cortical thickening in *Nigersaurus* is thus far from the degree expected, based on previous studies on heavy taxa. Complete cross-sections from the literature suggest a high variability in cortical thickening and presence of spongiosa in the shaft across sauropod taxa (i.e. far beyond the pattern observed in *Nigersaurus*), which does not appear to be related to size. Our results suggest that the microanatomical structure in sauropod limb bones was not subject to drastic selective pressures imposed by heavy weight-bearing. Instead, the columnar limb architecture, as well as some other external features, such as the presence of a fleshy pad and cartilaginous epiphyses may have been sufficient to support heavy weight, hence relaxing biomechanical pressures on microanatomy. This observation may also suggest that the mass increase in sauropods was lower than expected in relation to size increase, rejoining the conclusions of studies on postcranial pneumaticity, and tending to support the lowest body mass estimations made for sauropod taxa. More specifically, the pattern seen in *Nigersaurus* limb long bones is congruent with the lightened condition of the rest of its skeleton. The trends highlighted in this study would benefit from a more exhaustive exploration of microanatomical variability within sauropods, but also of other heavy terrestrial tetrapods, which will help us to better understand the evolution of limb bone microanatomy in relation to weight-bearing and to gigantism.

*Acknowledgements.* We warmly thank Marta Bellato for performing the scans and reconstructions at the AST-RX platform (UMS 2700, MNHN). We also thank Vincent Pernègre, Damien Olivier, Sandra Daillie, and Maxime Peretta for providing help and access to the MNHN collections, Cyril Etienne and Guillaume Houée for discussion on their preliminary work on rhinoceroses and tapirs, and Kévin Le Verger and Pierre Lamarche for their logistic help for this study. We also thank Ignacio Cerda (Museo Carlos Ameghino, Cipolletti, Argentina) and an anonymous reviewer for their constructive comments that improved the quality of this manuscript, as well as Stephan Lautenschlager (University of Birmingham, Birmingham, UK) for his scientific editorial work, and Sally Thomas (Technical Editor and Publications Officer, The Palaeontological Association, UK) for the technical review, editorial work and comments. This work was funded by the European Research Council and is part of the GRAVIBONE project (ERC-2016-STG-715300).

*Author contributions.* **Conceptualization** Rémi Lefebvre (RL), Ronan Allain (RA), Alexandra Houssaye (AH); **Data Curation** RL, RA, Marta Bellato (MB); **Formal Analysis** RL; **Funding Acquisition** AH; **Investigation** RL, AH, MB; **Methodology** RL, AH; **Project Administration** RL, RA, AH; **Resources** AH; **Supervision** RA, AH; **Validation** RL, RA, AH; **Visualization** RL; **Writing – Original Draft Preparation** RL; **Writing – Review & Editing** RL, RA, AH.

## DATA ARCHIVING STATEMENT

Raw scan data are archived at the Muséum national d'Histoire naturelle, Paris, France and registered on the 3Dtheque portal: https://3dtheque.mnhn.fr/.

*Editor.* Stephan Lautenschlager

## SUPPORTING INFORMATION

Additional Supporting Information can be found online (https://doi.org/10.1111/pala.12670):

**Table S1.** Cortical thickness in transverse sections figured in Houssaye *et al.* (2016), sorted by type of bone.

## REFERENCES


ALEXANDER, R. 1998. All-time giants: the largest animals and their problems. *Palaeontology*, **41**, 1231–1246.

AMSON, E. 2021. Humeral diaphysis structure across mammals. *Evolution*, **75**, 748–755.

AMSON, E. and KOLB, C. 2016. Scaling effect on the mid-diaphysis properties of long bones—the case of the Cervidae (deer). *The Science of Nature*, **103**, 58.

AMSON, E. and NYAKATURA, J. A. 2018. Palaeobiological inferences based on long bone epiphyseal and diaphyseal structure – the forelimb of xenarthrans (Mammalia). *bioRxiv*, 318121, v.5.

AMSON, E., de MUIZON, C., LAURIN, M., ARGOT, C. and de Buffrénil, V. 2014. Gradual adaptation of bone structure to aquatic lifestyle in extinct sloths from Peru. *Proceedings of the Royal Society B*, **281**, 20140192.

AUGAT, P. and SCHORLEMMER, S. 2006. The role of cortical bone and its microstructure in bone strength. *Age & Ageing*, **35**, ii27–ii31.

AURELIANO, T., GHILARDI, A. M., NAVARRO, B. A., FERNANDES, M. A., RICARDI-BRANCO, F. and WEDEL, M. J. 2021. Exquisite air sac histological traces in a hyperpneumatized nanoid sauropod dinosaur from South America. *Scientific Reports*, **11**, 1–9.

BATES, K. T., FALKINGHAM, P. L., MACAULAY, S., BRASSEY, C. and MAIDMENT, S. C. 2015. Downsizing a giant: re-evaluating *Dreadnoughtus* body mass. *Biology Letters*, **11**, 20150215.

BONNAN, M. F., SANDRIK, J. L., NISHIWAKI, T., WILHITE, D. R., ELSEY, R. M. and VITTORE, C. 2010. Calcified cartilage shape in archosaur long bones reflects overlying joint shape in stress-bearing elements: implications for nonavian dinosaur locomotion. *The Anatomical Record*, **293**, 2044–2055.

BONNAN, M. F., WILHITE, D. R., MASTERS, S. L., YATES, A. M., GARDNER, C. K. and AGUIAR, A. 2013. What lies beneath: sub-articular long bone shape scaling in eutherian mammals and saurischian dinosaurs suggests different locomotor adaptations for gigantism. *PLoS One*, **8**, e75216.

CAMPIONE, N. E. 2017. Extrapolating body masses in large terrestrial vertebrates. *Paleobiology*, **43**, 693–699.

CAMPIONE, N. E. and EVANS, D. C. 2020. The accuracy and precision of body mass estimation in non-avian dinosaurs. *Biological Reviews*, **95**, 1759–1797.

CANOVILLE, A. and LAURIN, M. 2010. Evolution of humeral microanatomy and lifestyle in amniotes, and some comments on palaeobiological inferences. *Biological Journal of the Linnean Society*, **100**, 384–406.

CANOVILLE, A., CHINSAMY, A. and ANGST, D. 2022. New comparative data on the long bone microstructure of large extant and extinct flightless birds. *Diversity*, **14**, 298.

CARRANO, M. T. 2001. Implications of limb bone scaling, curvature and eccentricity in mammals and non-avian dinosaurs. *Journal of Zoology*, **254**, 41–55.

CARRANO, M. T. 2005. The evolution of sauropod locomotion: morphological diversity of a secondarily quadrupedal radiation. 229–249. *In* CURRY ROGERS, K. and WILSON, J. (eds) *The sauropods: Evolution and paleobiology*. University of California Press.

CERDA, I. A. 2022. South American sauropodomorphs: what their bone histology has revealed to us. 473–501. *In* OTERO, A., CARBALLIDO, J. L. and POL, D. (eds) *South American sauropodomorph dinosaurs: Record, diversity and evolution*. Springer.

CERDA, I. A., SALGADO, L. and POWELL, J. E. 2012. Extreme postcranial pneumaticity in sauropod dinosaurs from South America. *Paläontologische Zeitschrift*, **86**, 441–449.

CERDA, I. A., GARCÍA, R. A., POWELL, J. E. and LOPEZ, O. 2015. Morphology, microanatomy, and histology of titanosaur (Dinosauria, Sauropoda) osteoderms from the Upper Cretaceous of Patagonia. *Journal of Vertebrate Paleontology*, **35**, e905791.

CERDA, I. A., CHINSAMY, A., POL, D., APALDETTI, C., OTERO, A., POWELL, J. E. and MARTÍNEZ, R. N. 2017. Novel insight into the origin of the growth dynamics of sauropod dinosaurs. *PLoS One*, **12**, e0179707.

CHRISTIANSEN, P. 2007. Long-bone geometry in columnar-limbed animals: allometry of the proboscidean appendicular skeleton. *Zoological Journal of the Linnean Society*, **149**, 423–436.

CIGNONI, P., CALLIERI, M., CORSINI, M., DELLEPIANE, M., GANOVELLI, F. and RANZUGLIA, G. 2008. Meshlab: an open-source mesh processing tool. *Eurographics Italian Chapter Conference*, **2008**, 129–136.

COMPANY, J. 2011. Bone histology of the titanosaur *Lirainosaurus astibiae* (Dinosauria: Sauropoda) from the Latest Cretaceous of Spain. *Naturwissenschaften*, **98**, 67–78.

COOMBS, W. P. 1978. Theoretical aspects of cursorial adaptations in dinosaurs. *The Quarterly Review of Biology*, **53**, 393–418.

CURREY, J. D. and ALEXANDER, R. M. 1985. The thickness of the walls of tubular bones. *Journal of Zoology*, **206**, 453–468.

CURRY, K. 1999. Ontogenetic histology of *Apatosaurus* (Dinosauria: Sauropoda): new insights on growth rates and longevity. *Journal of Vertebrate Paleontology*, **19**, 654–665.

CURRY ROGERS, K. and KULIK, Z. 2018. Osteohistology of *Rapetosaurus krausei* (sauropoda: titanosauria) from the upper cretaceous of Madagascar. *Journal of Vertebrate Paleontology*, **38**, 1–24.

CURRY ROGERS, K., D'EMIC, M., ROGERS, R., VICKARYOUS, M. and CAGAN, A. 2011. Sauropod dinosaur osteoderms from the Late Cretaceous of Madagascar. *Nature Communications*, **2**, 1–5.

CURRY ROGERS, K., WHITNEY, M., D'EMIC, M. and BAGLEY, B. 2016. Precocity in a tiny titanosaur from the Cretaceous of Madagascar. *Science*, **352**, 450–453.

CURTIN, A. J., MACDOWELL, A. A., SCHAIBLE, E. G. and ROTH, V. L. 2012. Noninvasive histological comparison of bone growth patterns among fossil and extant neonatal elephantids using synchrotron radiation x-ray microtomography. *Journal of Vertebrate Paleontology*, **32**, 939–955.

FABBRI, M., NAVALÓN, G., BENSON, R. B., POL, D., O'CONNOR, J., BHULLAR, B. A. S., ERICKSON, G. M., NORELL, M. A., ORKNEY, A., LAMANNA, M. C.,

ZOUHRI, S., BECKER, J., EMKE, A., DAL SASSO, C., BINDELLINI, G., MAGANUCO, S., AUDITORE, M. and IBRAHIM, N. 2022. Subaqueous foraging among carnivorous dinosaurs. *Nature*, **603**, 852–857.

GALTON, P. M. 2005. Bones of large dinosaurs (Prosauropoda and Stegosauria) from the Thaetic Bone Bed (Upper Triassic) of Aust Cliff, southwest England. *Revue de Paléobiologie*, **24**, 51–74.

GHILARDI, A. M., AURELIANO, T., DUQUE, R. R., FERNANDES, M. A., BARRETO, A. M. and CHINSAMY, A. 2016. A new titanosaur from the Lower Cretaceous of Brazil. *Cretaceous Research*, **67**, 16–24.

GONZÁLEZ, R., GALLINA, P. A. and CERDA, I. A. 2017. Multiple paleopathologies in the dinosaur *Bonitasaura salgadoi* (Sauropoda: Titanosauria) from the Upper Cretaceous of Patagonia, Argentina. *Cretaceous Research*, **79**, 159–170.

GONZÁLEZ, R., CERDA, I. A., FILIPPI, L. S. and SALGADO, L. 2020. Early growth dynamics of titanosaur sauropods inferred from bone histology. *Palaeogeography, Palaeoclimatology, Palaeoecology*, **537**, 109404.

GREGORY, W. K. 1912. Notes on the principles of quadrupedal locomotion and on the mechanism of the limbs in hoofed animals. *Annals of the New York Academy of Sciences*, **22**, 267–292.

HAN, F., ZHAO, Q., STIEGLER, J. and XU, X. 2020. Bone histology of the non-iguanodontian ornithopod *Jeholosaurus shangyuanensis* and its implications for dinosaur skeletochronology and development. *Journal of Vertebrate Paleontology*, **40**, e1768538.

HATCHER, J. B. 1901. *Diplodocus* (Marsh): its osteology, taxonomy, and probable habits, with a restoration of the skeleton. *Memoirs of the Carnegie Museum*, **1**, 1–63.

HEDRICK, B. P., TUMARKIN-DERATZIAN, A. R. and DODSON, P. 2014. Bone microstructure and relative age of the holotype specimen of the diplodocoid sauropod dinosaur *Suuwassea emilieae*. *Acta Palaeontologica Polonica*, **59**, 295–304.

HEINRICH, R. E., RUFF, C. B. and WEISHAMPEL, D. B. 1993. Femoral ontogeny and locomotor biomechanics of *Dryosaurus lettowvorbecki* (Dinosauria, Iguanodontia). *Zoological Journal of the Linnean Society*, **108**, 179–196.

HENDERSON, D. M. 2006. Burly gaits: centers of mass, stability, and the trackways of sauropod dinosaurs. *Journal of Vertebrate Paleontology*, **26**, 907–921.

HILDEBRAND, M. 1982. *Analysis of vertebrate structure*. John Wiley & Sons.

HOLLIDAY, C. M., RIDGELY, R. C., SEDLMAYR, J. C. and WITMER, L. M. 2010. Cartilaginous epiphyses in extant archosaurs and their implications for reconstructing limb function in dinosaurs. *PLoS One*, **5**, e13120.

HOUSSAYE, A. and BOTTON-DIVET, L. 2018. From land to water: evolutionary changes in long bone microanatomy of otters (Mammalia: Mustelidae). *Biological Journal of the Linnean Society*, **125**, 240–249.

HOUSSAYE, A. and PRÉVOTEAU, J. 2020. What about limb long bone nutrient canal(s)? – a 3D investigation in mammals. *Journal of Anatomy*, **236**, 510–521.

HOUSSAYE, A., TAFFOREAU, P., de MUIZON, C. and GINGERICH, P. D. 2015. Transition of Eocene whales from land to sea: evidence from bone microstructure. *PLoS One*, **10**, e0118409.

HOUSSAYE, A., WASKOW, K., HAYASHI, S., CORNETTE, R., LEE, A. H. and HUTCHINSON, J. R. 2016. Biomechanical evolution of solid bones in large animals: a microanatomical investigation. *Biological Journal of the Linnean Society*, **117**, 350–371.

HOUSSAYE, A., TAVERNE, M. and CORNETTE, R. 2018. 3D quantitative comparative analysis of long bone diaphysis variations in microanatomy and cross-sectional geometry. *Journal of Anatomy*, **232**, 836–849.

HOUSSAYE, A., MARTIN, F., BOISSERIE, J.-R. and LIHOREAU, F. 2021. Paleoecological inferences from long bone microanatomical specializations in Hippopotamoidea (Mammalia, Artiodactyla). *Journal of Mammalian Evolution*, **28**, 847–870.

HUTCHINSON, J. R. 2021. The evolutionary biomechanics of locomotor function in giant land animals. *Journal of Experimental Biology*, **224**, 217463.

IBIRICU, L. M., LAMANNA, M. C., MARTINEZ, R. D., CASAL, G. A., CERDA, I. A., MARTINEZ, G. and SALGADO, L. 2017. A novel form of postcranial skeletal pneumaticity in a sauropod dinosaur: implications for the paleobiology of Rebbachisauridae. *Acta Palaeontologica Polonica*, **62**, 221–237.

JANNEL, A., NAIR, J. P., PANAGIOTOPOULOU, O., ROMILIO, A. and SALISBURY, S. W. 2019. "Keep your feet on the ground": simulated range of motion and hind foot posture of the Middle Jurassic sauropod *Rhoetosaurus brownei* and its implications for sauropod biology. *Journal of Morphology*, **280**, 849–878.

JANNEL, A., SALISBURY, S. W. and PANAGIOTOPOULOU, O. 2022. Softening the steps to gigantism in sauropod dinosaurs through the evolution of a pedal pad. *Science Advances*, **8** (31), eabm8280.

JENTGEN-CESCHINO, B., STEIN, K. and FISCHER, V. 2020. Case study of radial fibrolamellar bone tissues in the outer cortex of basal sauropods. *Philosophical Transactions of the Royal Society B*, **375**, 20190143.

KLEIN, N. and SANDER, M. 2008. Ontogenetic stages in the long bone histology of sauropod dinosaurs. *Paleobiology*, **34**, 247–263.

KLEIN, N., CHRISTIAN, A. and SANDER, P. M. 2012a. Histology shows that elongated neck ribs in sauropod dinosaurs are ossified tendons. *Biology Letters*, **8**, 1032–1035.

KLEIN, N., SANDER, P. M., STEIN, K., LE LOEUFF, J., CARBALLIDO, J. L. and BUFFETAUT, E. 2012b. Modified laminar bone in *Ampelosaurus atacis* and other titanosaurs (Sauropoda): implications for life history and physiology. *PLoS One*, **7**, e36907.

LAURIN, M., CANOVILLE, A. and GERMAIN, D. 2011. Bone microanatomy and lifestyle: a descriptive approach. *Comptes Rendus Palevol*, **10**, 381–402.

LEFEBVRE, R., ALLAIN, R., HOUSSAYE, A. and CORNETTE, R. 2020. Disentangling biological variability and taphonomy: shape analysis of the limb long bones of the sauropodomorph dinosaur *Plateosaurus*. *PeerJ*, **8**, e9359.

LEFEBVRE, R., HOUSSAYE, A., MALLISON, H., CORNETTE, R. and ALLAIN, R. 2022. A path to

gigantism: three-dimensional study of the sauropodomorph limb long bone shape variation in the context of the emergence of the sauropod bauplan. *Journal of Anatomy*, **241**, 297–336.

LEGENDRE, L. J. and BOTHA-BRINK, J. 2018. Digging the compromise: investigating the link between limb bone histology and fossoriality in the aardvark (*Orycteropus afer*). *PeerJ*, **6**, e5216.

MALLET, C., CORNETTE, R., BILLET, G. and HOUSSAYE, A. 2019. Interspecific variation in the limb long bones among modern rhinoceroses—extent and drivers. *PeerJ*, **7**, e7647.

MALLISON, H. 2010. CAD assessment of the posture and range of motion of *Kentrosaurus aethiopicus* Hennig 1915. *Swiss Journal of Geosciences*, **103**, 211–233.

MILNE, N. 2016. Curved bones: an adaptation to habitual loading. *Journal of Theoretical Biology*, **407**, 18–24.

MITCHELL, J. and SANDER, P. M. 2014. The three-front model: a developmental explanation of long bone diaphyseal histology of Sauropoda. *Biological Journal of the Linnean Society*, **112**, 765–781.

NAKAJIMA, Y., HIRAYAMA, R. and ENDO, H. 2014. Turtle humeral microanatomy and its relationship to lifestyle. *Biological Journal of the Linnean Society*, **112**, 719–734.

NGANVONGPANIT, K., SIENGDEE, P., BUDDHACHAT, K., BROWN, J. L., KLINHOM, S., PITAKARNNOP, T., ANGKAWANISH, T. and THITARAM, C. 2017. Anatomy, histology and elemental profile of long bones and ribs of the Asian elephant (*Elephas maximus*). *Anatomical Science International*, **92**, 554–568.

OSBORN, H. F. 1900. The angulation of the limbs of proboscidia, dinocerata, and other quadrupeds, in adaptation to weight. *The American Naturalist*, **34**, 89–94.

OSBORN, H. F. 1929. *The titanotheres of ancient Wyoming, Dakota, and Nebraska*. Government Printing Office, Washington, DC.

OSTROM, J. and McINTOSH, J. 1966. *Marsh's dinosaurs: The collections from Como Bluff*. Yale University Press.

OXNARD, C. 1990. From giant ground sloths to human osteoporosis: an essay on the architecture and biomechanics of bone. 75–96. *In* FREEDMAN, L. (ed.) *Is our future limited by our past?* Proceedings of the Australasian Society for Human Biology, **3**. The Centre for Human Biology, University of Western Australia Nedlands.

de RICQLÈS, A. 1983. Cyclical growth in the long limb bones of a sauropod dinosaur. *Acta Palaeontologica Polonica*, **28**, 225–232.

RIMBLOT-BALY, F., de RICQLÈS, A. and ZYLBERBERG, L. 1995. Analyse paléohistologique d'une série de croissance partielle chez *Lapparentosaurus madagascariensis* (Jurassique moyen): essai sur la dynamique de croissance d'un dinosaure sauropode. *Annales de Paleontologie*, **81**, 49–86.

SALGADO, L., CORIA, R. A. and CALVO, J. O. 1997. Evolution of titanosaurid sauropods: phylogenetic analysis based on the postcranial evidence. *Ameghiniana*, **34**, 3–32.

SANDER, P. M. 2000. Longbone histology of the Tendaguru sauropods: implications for growth and biology. *Paleobiology*, **26**, 466–488.

SANDER, P. M. and CLAUSS, M. 2008. Sauropod gigantism. *Science*, **322**, 200–201.

SANDER, P. M., MATEUS, O., LAVEN, T. and KNÖTSCHKE, N. 2006. Bone histology indicates insular dwarfism in a new Late Jurassic sauropod dinosaur. *Nature*, **441**, 739–741.

SANDER, P. M., KLEIN, N., STEIN, K. and WINGS, O. 2011. Sauropod bone histology and its implications for sauropod biology. 276–302. *In* KLEIN, N., REMES, K., GEE, C. T. and SANDER, P. M. (eds) *Biology of the sauropod dinosaurs: Understanding the life of giants*. Indiana University Press.

SCHNEIDER, C. A., RASBAND, W. S. and ELICEIRI, K. W. 2012. NIH Image to ImageJ: 25 years of image analysis. *Nature Methods*, **9**, 671–675.

SCHWARZ, D., WINGS, O. and MEYER, C. A. 2007. Super sizing the giants: first cartilage preservation at a sauropod dinosaur limb joint. *Journal of the Geological Society*, **164**, 61–65.

SERENO, P. C., BECK, A. L., DUTHEIL, D. B., LARSSON, H. C., LYON, G. H., MOUSSA, B., SADLEIR, R. W., SIDOR, C. A., VARRICCHIO, D. J. and WILSON, G. P. 1999. Cretaceous sauropods from the Sahara and the uneven rate of skeletal evolution among dinosaurs. *Science*, **286**, 1342–1347.

SERENO, P. C., WILSON, J. A., WITMER, L. M., WHITLOCK, J. A., MAGA, A., IDE, O. and ROWE, T. A. 2007. Structural extremes in a Cretaceous dinosaur. *PLoS One*, **2**, e1230.

STEIN, K., CSIKI, Z., ROGERS, K. C., WEISHAMPEL, D. B., REDELSTORFF, R., CARBALLIDO, J. L. and SANDER, P. M. 2010. Small body size and extreme cortical bone remodeling indicate phyletic dwarfism in *Magyarosaurus dacus* (Sauropoda: Titanosauria). *Proceedings of the National Academy of Sciences*, **107**, 9258–9263.

STRAEHL, F. R., SCHEYER, T. M., FORASIEPI, A. M., MACPHEE, R. D. and SÁNCHEZ-VILLAGRA, M. R. 2013. Evolutionary patterns of bone histology and bone compactness in xenarthran mammal long bones. *PLoS One*, **8**, e69275.

SULEJ, T. and NIEDŹWIEDZKI, G. 2019. An elephant-sized Late Triassic synapsid with erect limbs. *Science*, **363**, 78–80.

TAQUET, P. 1976. Géologie et paléontologie du gisement de Gadoufaoua (Aptien du Niger). *Cahiers de Paléontologie*, 1–191.

TSAI, H. P. and HOLLIDAY, C. M. 2014. Articular soft tissue anatomy of the archosaur hip joint: structural homology and functional implications. *Journal of Morphology*, **276**, 601–630.

TSAI, H. P., MIDDLETON, K. M., HUTCHINSON, J. R. and HOLLIDAY, C. M. 2020. More than one way to be a giant: convergence and disparity in the hip joints of saurischian dinosaurs. *Evolution*, **74**, 1654–1681.

VIDAL, D., ORTEGA, F., GASCÓ, F., SERRANO-MARTÍNEZ, A. and SANZ, J. L. 2017. The internal anatomy of titanosaur osteoderms from the Upper Cretaceous of Spain is compatible with a role in oogenesis. *Scientific Reports*, **7**, 1–11.

VOEGELE, K. K., SIEGLER, S., BONNAN, M. F. and LACOVARA, K. J. 2022. Constraining morphologies of soft tissues in extinct vertebrates using multibody dynamic simulations: a case study on articular cartilage of the sauropod *Dreadnoughtus*. *Frontiers in Earth Science*, **10**, 786247.

WALL, W. P. 1983. The correlation between high limb-bone density and aquatic habits in recent mammals. *Journal of Paleontology*, **57**, 197–207.

WARNER, S. E., PICKERING, P., PANAGIOTOPOULOU, O., PFAU, T., REN, L. and HUTCHINSON, J. R. 2013. Size-related changes in foot impact mechanics in hoofed mammals. *PLoS One*, **8**, e54784.

WASKOW, K. and SANDER, P. M. 2014. Growth record and histological variation in the dorsal ribs of *Camarasaurus* sp. (Sauropoda). *Journal of Vertebrate Paleontology*, **34**, 852–869.

WEDEL, M. J. 2003. The evolution of vertebral pneumaticity in sauropod dinosaurs. *Journal of Vertebrate Paleontology*, **23**, 344–357.

WEDEL, M. J. 2005. Postcranial skeletal pneumaticity in sauropods and its implications for mass estimates. 201–228. *In* CURRY ROGERS, K. and WILSON, J. A. (eds) *The sauropods: Evolution and paleobiology*. University of California Press.

WEISSENGRUBER, G., EGGER, G., HUTCHINSON, J., GROENEWALD, H. B., ELSÄSSER, L., FAMINI, D. and FORSTENPOINTNER, G. 2006. The structure of the cushions in the feet of African elephants (*Loxodonta africana*). *Journal of Anatomy*, **209**, 781–792.

WILLIE, B. M., ZIMMERMANN, E. A., VITIENES, I., MAIN, R. P. and KOMAROVA, S. V. 2020. Bone adaptation: safety factors and load predictability in shaping skeletal form. *Bone*, **131**, 115114.

WILSON, J. A. 2005. Integrating ichnofossil and body fossil records to estimate locomotor posture and spatiotemporal distribution of early sauropod dinosaurs: a stratocladistic approach. *Paleobiology*, **31**, 400–423.

WILSON, J. A. and ALLAIN, R. 2015. Osteology of *Rebbachisaurus garasbae* Lavocat, 1954, a diplodocoid (Dinosauria, Sauropoda) from the early Late Cretaceous–aged Kem Kem beds of southeastern Morocco. *Journal of Vertebrate Paleontology*, **35**, e1000701.

WINGS, O., SANDER, P. M., TÜTKEN, T., FOWLER, D. W. and SUN, G. 2007. Growth and life history of Asia's largest dinosaur. *Journal of Vertebrate Paleontology*, **27**, 167A.

WOODWARD, H. N. and LEHMAN, T. M. 2009. Bone histology and microanatomy of *Alamosaurus sanjuanensis* (Sauropoda: Titanosauria) from the maastrichtian of Big Bend National Park, Texas. *Journal of Vertebrate Paleontology*, **29**, 807–821.

YATES, A. M., WEDEL, M. J. and BONNAN, M. F. 2012. The early evolution of postcranial skeletal pneumaticity in sauropodomorph dinosaurs. *Acta Palaeontologica Polonica*, **57**, 85–100.

YE, Y., PENG, G. and JIANG, S. 2007. Preliminary histological study on the long bones of Middle Jurassic *Shunosaurus* and *Omeisaurus* from Dashanpu, Zigong, Sichuan. *Acta Palaeontologica Sinica*, **46**, 135–144.